

PAPER • OPEN ACCESS

## Polarization Based Out-Coupling for Cavity Based X-ray FELs

To cite this article: Patrick Rauer 2024 *J. Phys.: Conf. Ser.* **2687** 032014

View the [article online](#) for updates and enhancements.

You may also like

- [Near-surface structural study of transition metal oxides to understand their electronic properties](#)  
Yusuke Wakabayashi
- [Synthesis of Flower-Like Iron Oxide Capped Tripolyphosphate for Electrochemical Detection of Carbadox Drugs in Meat](#)  
Arumugam Sangili, Muthaiah Annalakshmi, Shen-Ming Chen et al.
- [Graded circular Bragg reflectors: a semi-analytical retrieval of approximate pitch profiles from Mueller-matrix data](#)  
Arturo Mendoza-Galván, Kenneth Järrendahl and Hans Arwin



**UNITED THROUGH SCIENCE & TECHNOLOGY**

 **The Electrochemical Society**  
Advancing solid state & electrochemical science & technology

**248th  
ECS Meeting**  
Chicago, IL  
October 12-16, 2025  
*Hilton Chicago*

**Science +  
Technology +  
YOU!**

**Register by  
September 22  
to save \$\$**

**REGISTER NOW**

# Polarization Based Out-Coupling for Cavity Based X-ray FELs

**Patrick Rauer**

Deutsches Elektronen-Synchrotron DESY, Germany

E-mail: [patrick.rauer@desy.de](mailto:patrick.rauer@desy.de)

**Abstract.** Cavity Based X-ray Free-Electron Lasers (CBXFELs) promise fully 3D coherent, very brilliant and shot-to-shot stable X-ray pulses. For CBXFELs the X-ray radiation is trapped in an X-ray optical cavity, which is formed using Bragg-reflecting crystal mirrors. As is the case for laser systems in the optical regime, a major question for the CBXFELs is how to couple out the radiation from the cavity. Possibilities range from employing semi-transparent thin crystals, over manipulation of the electron phase space density to cavity dumping schemes. In this work, making use of the strong polarization of Bragg reflection shall be studied for out-coupling. As the radiation does not change its polarization during Bragg reflection, reflection in the direction of the polarization vector is suppressed. By adjusting the 3D orientation of the crystals with respect to the polarization axis of a linearly polarized undulator, or vice versa, the transmission through the crystals can be tailored to some degree independently of the crystal thickness.

## 1. Introduction

Due to the lack of monochromatic external seeding sources in the hard X-ray regime, current hard X-ray Free-Electron Laser (XFEL) machines such as the *Linac Coherent Light Source* (LCLS), the *European XFEL* (EuXFEL), the *Spring-8 Angstrom Compact free-electron LASer* (SACLA), the SwissFEL and the *Pohang Accelerator Laboratory X-ray Free Electron Laser* (PAL-XFEL) are mainly using the seedless self-amplified spontaneous emission (SASE) scheme for operation. These sources produce very brilliant femtosecond X-ray pulses with a high degree of transverse coherence. Being initiated from the statistical noise of spontaneous emission, they do, however, suffer from a low degree of longitudinal coherence, with a typical radiation pulse of some 10femtoseconds length, consisting of thousands of longitudinal modes, as well as a strong shot-to-shot fluctuations. A promising class of schemes still to be realized are the Cavity Based X-ray FELs. This term includes both the high-gain *X-ray Regenerative Amplifier FEL* (XRAFEL) proposed by *Z. Huang* in 2006 [1] as well as the low-gain *X-ray Free Electron Laser Oscillator* (XFELo) proposed by *K.J. Kim* in 2008 [2]. The fundamental commonality of these schemes are that they are based on trapping FEL radiation inside a X-ray optical cavity, using monochromatizing crystals based on Bragg reflection instead of total reflecting optical mirrors. Due to the promise of delivering outstanding radiation properties, CBXFELs have received growing interest in the recent years [3, 4, 5, 6, 7, 8, 9, 10, 11, 12, 13, 14]. Currently, there are two projects to install proof-of-concepts CBXFEL experiments at the European XFEL [15] and the *Linac Coherent Light Source-II* (LCLS-II) [16], respectively. Also, at the still to be completed *Shanghai High-Repetition-Rate XFEL and Extreme Light Facility* (SHINE) a full cavity enhanced FEL beamline is planned [17].



Same as for optical laser cavities, a major challenge of CBXFELs is how to efficiently couple out the radiation. The options to do that range from X-ray optics based techniques (see for example [18, 19, 13, 12]) to electron beam based ones (see for example [1, 20, 21, 14]). In this contribution, the use of the strong polarization dependence of Bragg reflection is studied as an X-ray optics based approach for radiation out-coupling, applicable both to low-gain XFEL sources, requiring low cavity losses, as for high-gain XRFEL sources, which can take advantage of high out-coupling rates.

## 2. Polarization dependence of dynamic diffraction

For the calculation of the reflection efficiency at the crystals, dynamic diffraction theory is applied throughout this contribution. In order to keep the algebra as simple as possible, a couple of approximations are applied, which are well justified for the perspective crystal used in CBXFELs. First, the two beam approximation is applied, meaning that the reflection condition is only met for one single set  $\vec{H}$  of parallel crystal planes. Second, the angle of incidence is assumed to be much bigger than 0, neglecting grazing incidence. Third, only symmetric Bragg (backward) reflection is considered, meaning that the surface of the crystal and the reflecting planes are the same, which cancels possible dispersion. And lastly, the crystal itself is assumed to be perfect and not-strained, which strongly simplifies the algebra<sup>1</sup>.

Generally, the system of equations for the dynamic diffraction is dependent on the polarization. A convenient orthonormal basis set for polarization of the incoming beam with wavevector  $\vec{K}_0$  and for the reflected beam with wavevector  $\vec{K}_H = \vec{K}_0 + \vec{H}$  is [22]

$$\hat{\sigma} = \hat{\sigma}_0 = \hat{\sigma}_H = \frac{\vec{H} \times \vec{K}_0}{|\vec{H} \times \vec{K}_0|}, \quad \hat{\pi}_{0,H} = \frac{\vec{K}_{0,H} \times \hat{\sigma}}{|\vec{K}_{0,H}|}. \quad (1)$$

This choice of basis perfectly decouples the polarization components  $\hat{\sigma}$  and  $\hat{\pi}$  from each other. Then, the reflectivity  $r_{\sigma,\pi}$  and transmissivity  $t_{\sigma,\pi}$  for a crystal of thickness  $t_c$  at wavelength  $\lambda$  and, hence, wavenumber  $k = |\vec{K}_0| = 2\pi/\lambda$ , and Bragg angle  $\Theta_B = \arcsin(-\vec{K}_0 \vec{H}/k|\vec{H}|)$  become [22]

$$r_{\sigma,\pi} = R_+ R_- \frac{1 - e^{-i \frac{k}{2 \sin(\Theta_B)} (\epsilon_- - \epsilon_+) t_c}}{R_- - R_+ e^{-i \frac{k}{2 \sin(\Theta_B)} (\epsilon_- - \epsilon_+) t_c}}, \quad (2)$$

$$t_{\sigma,\pi} = e^{i \frac{k}{2 \sin(\Theta_B)} \epsilon_+ t_c} \frac{R_- - R_+}{R_- - R_+ e^{-i \frac{k}{2 \sin(\Theta_B)} (\epsilon_- - \epsilon_+) t_c}}, \quad (3)$$

$$\text{with } \epsilon_{\pm} = \frac{1}{2} \alpha \pm \sqrt{\frac{\alpha^2}{4} - \chi_0 \alpha + \chi_0^2 - P_{\sigma,\pi} |\chi_H|}$$

$$\text{and } \alpha = \frac{|\vec{H}|}{k} \left( \frac{|\vec{H}|}{k} - 2 \sin(\Theta_B) \right).$$

In above equations,  $\chi_{0,H}$  is the Fourier component of the material dependent susceptibility.  $P_{\sigma,\pi}$  a polarization dependent factor, which is  $P_{\sigma} = \hat{\sigma}_0 \hat{\sigma}_H = 1$  and  $P_{\pi} = \hat{\pi}_0 \hat{\pi}_H = \sin(2\Theta_B)$ . The strong dependence of  $P_{\pi}$  on the Bragg angle  $\Theta$  has a strong influence on the reflectivity and transmissivity and is the essential quantity for this study. This is emphasized in Fig. 1

<sup>1</sup> As the crystals employed for a CBXFEL source are chosen to be as perfect as possible to avoid beam degradation, this is a valid approximation for the start up of the seeding process. It does however break down if strong heating of the crystal occurs.

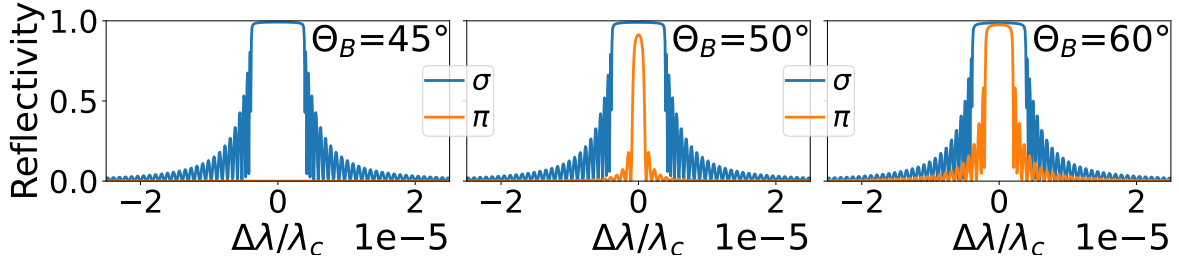


**Figure 1.** Spectral reflectivity  $R_{\sigma,\pi} = |r_{\sigma,\pi}|^2$  around the resonant wavelength for the  $\sigma$  and  $\pi$  incident polarization for three different Bragg angles. Unlike  $R_\sigma$ ,  $R_\pi$  shows a strong dependency on the Bragg angle, with  $R_\pi = 0$  for  $\Theta_B = 45^\circ$ . For  $|\Theta_B - 45^\circ| > 0$ , the peak reflectivity, but foremost the reflection bandwidth are effected. The calculations were done for a  $t_c = 100 \mu\text{m}$  thick diamond with  $\langle 1\ 0\ 0 \rangle$  surface orientation.

For the following, we assume a linearly polarized incoming radiation pulse  $\vec{E}_{in}(r, \lambda) = E_{in}(r, \lambda)\hat{x}$  from planar undulators in spectral domain, where without loss of generality the polarization is assumed in x-direction. Also, it is approximated that the cavity is, other than the crystals, only made up out of linear, lossless elements and that the reflection is independent of the higher order transverse moments of the pulse like divergence and width. Then it is sufficient for this study to look at the spectral components  $\vec{S}(\lambda)$ .  $\lambda$  will be omitted in the following. For a four crystal cavity of constant Bragg angle  $\Theta_B$

$$\begin{aligned}\vec{S}_{\text{seed}} &= S_{in} \begin{pmatrix} r_\sigma^4(\hat{x}\hat{\sigma})^2 + r_\pi^4(\hat{x}\hat{\pi})^2 \\ (\hat{x}\hat{\sigma}) (\hat{x}\hat{\pi}) (r_\pi^4 - r_\sigma^4) \end{pmatrix} \begin{pmatrix} \hat{x} \\ \hat{y} \end{pmatrix}, \\ \vec{S}_{\text{tr}} &= S_{in} \begin{pmatrix} t_\sigma(\hat{x}\hat{\sigma})^2 + t_\pi(\hat{x}\hat{\pi})^2 \\ (\hat{x}\hat{\sigma}) (\hat{x}\hat{\pi}) (t_\pi - t_\sigma) \end{pmatrix} \begin{pmatrix} \hat{x} \\ \hat{y} \end{pmatrix}\end{aligned}\quad (4)$$

are the radiation reentering the undulator as seed and the radiation transmitted through the first undulator, respectively. Above relations show, that not only the magnitude of reflection and transmission are effected by the polarization, but also the polarization of the seed and of the transmitted pulse can be rotated. While for the transmission this should not matter for most experiments, for the seeding radiation the y-component does not couple to the FEL process in the planar undulator and does, thus, not contribute to the seeding. Hence, we term it "lost" in the following.

In order to be more quantitative, the coordinate system of the undulators needs to be set into relation with the crystal coordinate system. For the undulator system, the downstream propagation direction of the radiation is set as  $\hat{z}_U$  and the polarization as  $\hat{x}_U$ . For the crystal coordinate system, the vector  $H$  is defined as parallel to  $-\hat{z}_C$  and the  $\hat{x}_C$  and  $\hat{y}_C$  coordinates can be chosen as random orthonormal vectors. The coordinate transformation can be set by forms of a rotation matrix with two rotational degrees of freedom around the  $\hat{x}_C$  and  $\hat{y}_C$  axis<sup>2</sup>, respectively called pitch and roll in the following, equivalent to a mechanical rotation setup. Then the transformation matrix from the crystal to the undulator frame becomes

$$R_C^U = \begin{pmatrix} \cos(R) & 0 & \sin(R) \\ \sin(R)\cos(P) & \sin(P) & -\cos(P)\cos(R) \\ -\sin(R)\sin(P) & \cos(P) & \sin(P)\cos(R) \end{pmatrix},$$

<sup>2</sup> For symmetric diffraction in the two-beam approximation, the rotation around the crystal  $\hat{z}$  axis has no impact on the diffraction and can be, hence, omitted.

where for pitch  $P = 90^\circ$  and roll  $R = 0$  the crystal and undulator coordinate systems coincide. Using this transformation, Eq. (4) becomes

$$\vec{S}_{\text{seed,tr}} = \frac{\vec{S}_{\text{in}}}{\sqrt{\cos^2(R) \cos^2(P) + \sin^2(R)}} \begin{pmatrix} \cos^2(P) \cos^2(R) a_\sigma(f) + \sin^2(R) a_\pi(f) \\ \cos(P) \cos(R) \sin(R) (a_\pi - a_\sigma) \end{pmatrix} \begin{pmatrix} \hat{x}_U \\ \hat{y}_U \end{pmatrix}, \quad (5)$$

with  $a_{\sigma,\pi} = r_{\sigma,\pi}^4$  for refl and  $t_{\sigma,\pi}$  for tr.

### 3. Efficiency of polarization based out-coupling

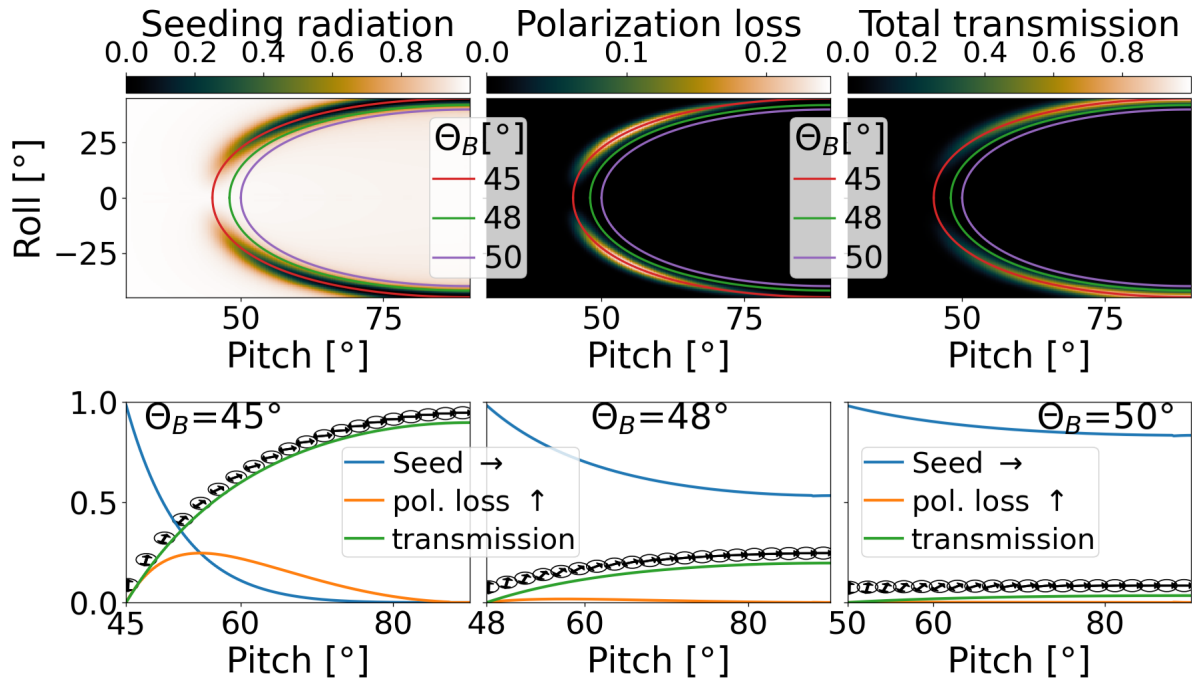


**Figure 2.** The top row shows the seeding efficiency  $\vec{S}_{\text{seed}} \hat{x}_U / |S_{\text{in}}|$ , the polarization loss  $\vec{S}_{\text{seed}} \hat{y}_U / |S_{\text{in}}|$  and the transmission  $|S_{\text{tr}}| / |S_{\text{in}}|$ . The red, green, and purple lines in the top row display angular combinations with constant  $\Theta_B$ . These lines correspond to the plots in the bottom row, where the roll is varied along with the pitch to yield  $\cos(R) = \sin(P) / \sin(\Theta_B)$ . On top of the green transmission line in the bottom plot the actual polarization directions of the transmitted radiation are sketched.

Figure 2 displays the effective seeding radiation  $\vec{S}_{\text{seed}} \hat{x}_U / |S_{\text{in}}|$ , 'lost' radiation  $\vec{S}_{\text{seed}} \hat{y}_U / |S_{\text{in}}|$  and transmitted radiation  $|S_{\text{tr}}| / |S_{\text{in}}|$  for a scan of angles. In the top row, a full angular scan over both pitch and roll is shown, while in the bottom row the angles are moved along one of the lines depicted in the top row, keeping the Bragg angle fixed to a specific value. The calculations were done for a comparably thick  $t_c = 100 \mu\text{m}$  diamond with  $\langle 100 \rangle$  surface orientation<sup>3</sup>, which is the crystal of choice for the European XFEL CBXFEL experiment [20]. From the transmission plot in the top right as well as the green lines in the bottom row, we see that the out-coupling technique is very sensitive to the Bragg angle, in accordance with the dependence

<sup>3</sup> The calculations presented in Fig. 2 were done for the central resonance wavelength of the diffraction process, thus omitting the impact the change of the reflection bandwidth with  $P_\pi$  as presented in Fig. 1.

of the polarization factor  $P_\pi$  on  $\Theta_B$ , with the transmission quickly dropping when moving away from  $\Theta_B = 45^\circ$ . An interesting observation from the bottom row plots is, in accordance with Eq. (5), that when varying the angles along a constant  $\Theta_B$  line, not only the transmission fraction is effected but also the polarization direction.

The polarization loss plot in the top middle as well as the constant  $\Theta_B = 45^\circ$  plot in the bottom left show a major downside of the technique. In the cases of high transmission, also the polarization loss becomes very high, reaching fractions higher than  $\hat{S}_{\text{seed}}\hat{y}_U/|S_{\text{in}}| > 20\%$ . Especially for a rectangular cavity with  $\Theta_B = 45^\circ$ , when going for transmission  $|S_{\text{tr}}|/|S_{\text{in}}| \geq 40\%$ , the loss fraction actually becomes bigger then the seeding fraction. This makes the polarization based out-coupling approach rather ineffective for XRFEL type applications, where high out-coupling efficiency is ideal to cope with the high gain. It might still be interesting for demonstrator type setups due to its simplicity.

For low-gain XFEL type setups which require out-coupling efficiencies on the order of 5%, though, the out-coupling technique is appealing. For the  $\Theta_B = 45^\circ$  case, the seeding loss at  $|S_{\text{tr}}|/|S_{\text{in}}| = 5\%$  still amounts to  $|S_{\text{seed}}\hat{y}_U/|S_{\text{in}}| \approx 5\%$  and the total losses, also including transmission and absorption losses, is  $1 - |S_{\text{seed}}\hat{x}_U/|S_{\text{in}}| \approx 12\%$ , which is quite much, but might be tolerable. For  $\Theta_B$ s moving away from the  $45^\circ$  line, the fraction of polarization loss actually decreases. However, this is due to an increase of reflectivity  $r_\pi$ , which is having a much larger penetration depth and, hence, more absorption. Thus, the actual total loss fraction of seeding radiation is increasing with increasing  $\Theta_B$ . This can also be seen from Fig. 3. The figure also shows that the losses are strongly dependent on the crystal thickness, effecting the total absorption, when moving away from the rectangular type cavities at  $\Theta_B = 45^\circ$  for which  $r_\pi = 0$ . Also, by lowering the desired transmission, the loss fraction can also be decreased.

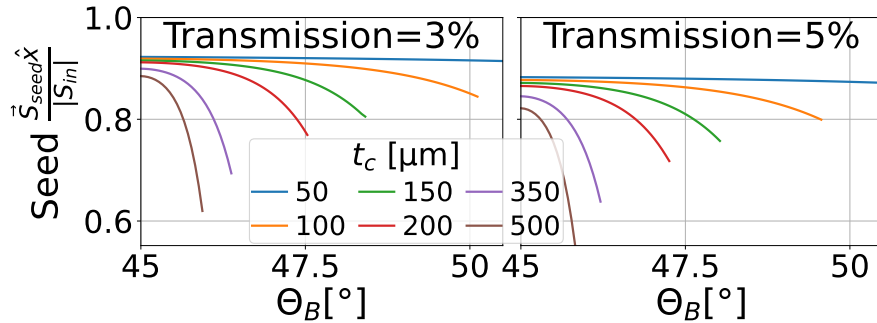


**Figure 3.** Seeding efficiencies  $|S_{\text{seed}}\hat{x}_U/|S_{\text{in}}| \approx 5\%$  against Bragg angle  $\Theta_B$  for various diamond thicknesses at two different desired transmission fractions. The end of a line signifies that the desired transmission cannot be achieved.

#### 4. Discussion and Outlook

Above analysis demonstrates that while the polarization based out-coupling can yield very high transmission fraction even with 'thick' crystals, it comes with the major downside of significant additional losses. It is clear that for the technique to be effective, it is important to stay very close or ideally on the  $\Theta_B = 45^\circ$  line. Nonetheless, compared to other out-coupling techniques of similar simplicity, in particular the sideband transmission initially used for the EuXFEL experiment [20] or thin drum head crystals, this downside can still be preferable to the decreased time-bandwidth product of the prior and the reduced mechanical stability of the latter method. As such, it might still be interesting for the rectangular  $\Theta_B = 45^\circ$  CBXFEL demonstrator at SLAC. Furthermore, it is possible to diminish the polarization loss problem by using hard X-ray crystal phase plates, for example made from diamond, as they are common

for synchrotron sources [23]. Using one phase retarder at the end of the undulators, in order to more easily manipulate the incoming polarization, and one retarder at the beginning, to turn the polarization back to obtain full seeding, the polarization based out-coupling could be majorly improved. This could make the technique also applicable to XRAFEL type sources. Another possibility to influence the polarization state without the necessity of tuning the crystal is the usage of variable polarization undulators (see for example [24]). This approach does however suffer from the same drawbacks as analyzed in the sections above.

Another small modification to adapt the concept to XRAFELs is to use a tapered afterburner with the polarization axes shifted by  $90^\circ$ . A similar approach has also been studied by *N. Huang et al.* [25] for polarization control of XFELs without concern for the out-coupling. For a rectangular cavity, the crystals could be aligned such that the first x-axis polarized undulator cells would be reflected by nearly 100%, while the y-axis polarized afterburner would be fully transmitted. By tuning the efficiency of the afterburner by a careful non-linear taper, as discussed in [25], one could tune the out-coupling rate and principally go to very high absolute transmission. However, as high pulse energies are being transmitted through the entire crystal and being absorbed on the way, high amounts of total heat are being deposited. This could strongly destabilize the CBXFEL source [20] and requires further studies.

### Acknowledgments

This work was funded by Deutsches Elektronen-Synchrotron (DESY). The numerical results were obtained using the Maxwell computational resources operated at Deutsches Elektronen-Synchrotron (DESY), Hamburg, Germany. I also want to thank Dr. Harald Sinn and Prof. Jörg Rossbach for useful discussion on the topic.

### References

- [1] Huang Z and Ruth R D 2006 *Physical Review Letters* **96** 144801
- [2] Kim K J, Shvyd'ko Y and Reiche S 2008 *Physical Review Letters* **100** 244802
- [3] Kim K J and Shvyd'ko Y V 2009 *Physical Review Special Topics - Accelerators and Beams* **12**
- [4] Lindberg R R, Kim K J, Shvyd'ko Y and Fawley W M 2011 *Physical Review Special Topics - Accelerators and Beams* **14**
- [5] Zemella J, Maag C P, Rossbach J, Sinn H and Tolkiehn M Numerical Simulations of an XFEL for the European XFEL driven by a Spent Beam *Proc. FEL'12* (JACoW Publishing, Geneva, Switzerland) pp 429–432 URL <https://jacow.org/FEL2012/papers/WEPD29.pdf>
- [6] Lindberg R R, Kim K J, Cai Y, Ding Y and Huang Z Transverse Gradient Undulators for a Storage Ring X-ray FEL Oscillator *Proc. FEL'13* (JACoW Publishing, Geneva, Switzerland) pp 740–748 URL <https://jacow.org/FEL2013/papers/THOBN002.pdf>
- [7] Adams B W and Kim K J 2015 *Physical Review Special Topics - Accelerators and Beams* **18**
- [8] Maxwell T J *et al.* Feasibility Study for an X-ray FEL Oscillator at the LCLS-II *Proc. IPAC'15* (JACoW Publishing, Geneva, Switzerland) pp 1897–1900 URL <https://jacow.org/IPAC2015/papers/TUPMA028.pdf>
- [9] Qin W *et al.* Start-to-End Simulations for an X-Ray FEL Oscillator at the LCLS-II and LCLS-II-HE *Proc. FEL'17* (JACoW Publishing, Geneva, Switzerland) pp 247–250 URL <https://jacow.org/fel2017/papers/TUC05.pdf>
- [10] Li K and Deng H 2018 *Nuclear Instruments and Methods in Physics Research - Section A* **895** 40–47
- [11] Rauer P, Bahns I, Decking W, Hillert W, Rossbach J and Sinn H 2019 Integration of an XFEL at the European XFEL facility *Proc. FEL'19*. (JACoW Publishing, Geneva, Switzerland) pp 62–65
- [12] Freund H P, van der Slot P J M and Shvyd'ko Y 2019 *New Journal of Physics* **21** 093028
- [13] Marcus G, Halavanau A, Huang Z, Krzywinski J, MacArthur J, Margraf R, Raubenheimer T and Zhu D 2020 *Physical Review Letters* **125** 254801
- [14] Margraf R A, MacArthur J P, Marcus G and Huang Z 2021 Microbunch Rotation as an Outcoupling Mechanism for Cavity-based X-Ray Free Electron Lasers *Proc. IPAC'20 (International Particle Accelerator Conference no 11)* (JACoW Publishing, Geneva, Switzerland) p 35 ISBN 978-3-95-450213-4 ISSN 2673-5490 URL <https://www.jacow.org/ipac2020/papers/WEVIR03.pdf>
- [15] Rauer P *et al.* 2023 *Phys. Rev. Accel. Beams* **26**(2) 020701

- [16] Marcus G *et al.* 2019 Cavity-based free-electron laser research and development: A joint argonne national laboratory and slac national laboratory collaboration *Proc. FEL'19* (JACoW Publishing, Geneva, Switzerland)
- [17] Huang N S *et al.* 2023 *Nuclear Science and Techniques* **34**
- [18] Kolodziej T, Vodnala P, Terentyev S, Blank V and Shvyd'ko Y 2016 *Journal of Applied Crystallography* **49** 1240–1244
- [19] Shvyd'ko Y 2019 *Physical Review Accelerators and Beams* **22** 100703
- [20] Rauer P, Decking W, Lipka D, Thoden D, Wohlenberg T, Bahns I, Brueggmann U, Casalbuoni S, Di Felice M, Dommach M, Grünert J, Karabekyan S, Koch A, La Civita D, Rio B, Samoylova L, Sinn H, Vannoni M, Youngman C, Hillert W and Rossbach J 2023 *Phys. Rev. Accel. Beams* **26**(2) 020701
- [21] Tang J, Duris J P, Marcus G and Marinelli A 2022 *Physical Review Accelerators and Beams* **25** 080701
- [22] Shvyd'ko Y 2004 *X-Ray Optics* (Springer Berlin Heidelberg) ISBN 3540214844
- [23] Hirano K, Ishikawa T and Kikuta S 1993 *Nuclear Instruments and Methods in Physics Research Section A: Accelerators, Spectrometers, Detectors and Associated Equipment* **336** 343–353
- [24] Bahrtdt J 2016 Shaping photon beams with undulators and wigglers *Synchrotron Light Sources and Free-Electron Lasers* (Springer International Publishing) pp 751–819
- [25] Huang N, Li K and Deng H 2020 **23** 030702